Published in Proceedings of NCSLI 2008 Workshop and Symposium (Boulder, CO: NCSLI, 2008), on CD

DESIGN AND PERFORMANCE OF THE NEW NIST HYBRID HUMIDITY GENERATOR

Speaker: Christopher Meyer
National Institute of Standards and Technology
100 Bureau Dr., Stop 8363, Gaithersburg, MD, 20899
phone: 301-975-4825, fax: 301-548-0206, email: cmeyer@nist.gov

Authors: C W Meyer, W W Miller, D C Ripple, and G E Scace
National Institute of Standards and Technology

Abstract

A new humidity generator has been constructed at the National Institute of Standards and Technology. Once fully operational, the NIST Hybrid Humidity Generator (HHG) will replace the Two-Pressure (2-P) Humidity Generator Mark II as the NIST primary humidity generation standard for frost/dew points from –70 °C to +25 °C using calibration gas-flow rates up to 150 standard liters per minute. The HHG will extend the NIST humidity generation range up to 85 °C, and is expected to outperform the 2-P Generator in terms of accuracy.

The HHG combines the two-pressure and divided-flow humidity generation techniques (hence the name "hybrid"). The centerpiece of the HHG is a heat-exchanger/saturator that is immersed in a temperature-controlled bath stable to within 1 mK. A precisely regulated pre-saturation process minimizes sensible and latent heat loading on the final saturator. For dew/frost point temperatures above –15 °C, the two-pressure principle is employed. For frost points at or below –15 °C, the water-vapor/air mixture is produced by mixing metered streams of moist air produced by the two-pressure principle with purified, dry air; here, the HHG saturates the wet air stream at a temperature close to the water triple point, reducing the uncertainty of the water vapor pressure. To our knowledge, this is the first primary generator that incorporates the divided-flow technique.

We describe here the design of the HHG as well as the estimated uncertainty of the dew/frost-point and mole fraction of moist air generated by it. The uncertainty estimate is based on a series of performance tests performed on the HHG. Finally, we include comparisons of the humidity generated by the HHG to that generated by the other NIST humidity-generation standards.

Published in Proceedings of NCSLI 2008 Workshop and Symposium (Boulder, CO: NCSLI, 2008), on CD

1. Introduction

The National Institute of Standards and Technology (NIST) has constructed a new primary standard humidity generator [1,2]. The facility is called the Hybrid Humidity Generator (HHG), and is so named because it incorporates the two-pressure and divided-flow humidity-generation principles [3] into a single design. This design is novel, as it is the first primary generator design that incorporates the divided-flow method. Once commissioned, it will replace the NIST Two-Pressure Humidity Generator Mark 2 [4,5] (known as the "2-P" generator) as the principal standard humidity generator for calibration of customer hygrometers. The NIST Low Frost-point Generator (LFPG) [6] will remain in operation as a complement to the HHG, being used primarily at frost-point temperatures below −70 °C. The HHG is designed to accommodate gas flows up to 150 L/min. The lower frost-point limit of the HHG is −70 °C, which is that of the 2-P generator. The higher dew-point limit of the HHG is 85 °C, which at ambient pressure corresponds to a water-vapor mole fraction of approximately 57 %. This limit is considerably higher than the 22 °C dew-point limit (2.6 % water-vapor mole fraction) of the 2-P generator. The increase in dew-point limit enables NIST to address the need of the semiconductor and fuel cell industries for high-range humidity standards. In addition, the humidity generated by the HHG has lower uncertainty than that from the 2-P generator. Finally, the HHG is easier, safer, and less expensive to operate than the 2-P generator. In this paper we discuss the design and performance of the generator and provide estimates of the uncertainty of the humidity in the gas generated from it.

2. Principle of Operation

Generation of gas with an accurately known moisture content starts with saturating the gas with water at a known temperature and pressure. Controlled saturation is accomplished by flowing a stream of the gas over a layer of water with a constant, uniform temperature until the gas is in thermodynamic equilibrium with the water. Ideally, the pressure of the gas is constant and pressure gradients within the gas are negligible. The mole fraction x of water vapor in the gas is then calculated using the equation

$$x = \frac{e(T_s)}{P_s} \; f(T_s, P_s) \qquad 1)$$

Here, T_s and P_s are the temperature and pressure of the gas and water in the saturator, and $e(T_s)$ is the water vapor pressure at T_s, as calculated by [7,8]. The enhancement factor $f(T_s, P_s)$ reflects departures from ideal solution behaviour and non-ideal gas effects [9].

At a given value of T_s, the HHG uses two methods (hence the name *hybrid*) to lower the humidity while still knowing its value accurately: the two-pressure technique and the divided-flow method. The two-pressure technique [3] involves saturating the gas at an elevated pressure and afterwards expanding the gas to a lower pressure. The divided-flow method [3], as used by the HHG, involves diluting the saturated gas with dry gas using precisely metered streams of gas. Such a technique allows generation of arbitrarily low humidity values while operating the

saturator at convenient temperatures. When performing hygrometer calibrations, the HHG uses the divided flow method for mole fractions less than 1.6×10^{-3} (frost points less than −15 °C).

3. Generator Design

A schematic representation of the layout of the HHG is shown in Figure 1. It involves a dry gas source, a two-pressure saturation system and a dilution system. For calibrations of relative-humidity sensors, the system incorporates a temperature-controlled test chamber in which the sensors are placed during calibration. The components of the HHG are described below.

The gas used in the HHG comes from the in-house supply of compressed air at NIST that has a pressure head of 550 kPa. Before entering the generator, the gas passes through a large regenerating gas dryer and CO_2 scrubber; this reduces the water mole fraction to 1×10^{-6} and removes 95% of the CO_2. After purification, the gas passes through a 240 L ballast tank which serves to minimize pressure pulses produced by the gas dryer. Computer-controlled mass flow controllers regulate the gas flow out from the tank; the maximum gas flow is 150 L/min.

The saturation system of the HHG consists of a pre-saturator and final saturator with a heatable tube connecting them. These parts are described below.

The pre-saturator accomplishes virtually all of the saturation, and the final saturator performs small adjustments to ensure that the generated humidity is constant and determinable with minimal uncertainty. The purpose of the pre-saturator is to allow the HHG to generate high water mole fractions with low uncertainty. For a thermodynamic generator to accomplish this, the dry carrier gas must be humidified to a dew-point temperature nearly equal to the final saturator temperature before entering the saturator. Since water vapor mole fractions in the HHG approach 0.57, operation without a pre-saturator would cause excessive latent heat loading on the final saturation process. This would introduce large temperature gradients in the final saturator, resulting in large uncertainties in the mole fraction of water in the gas.

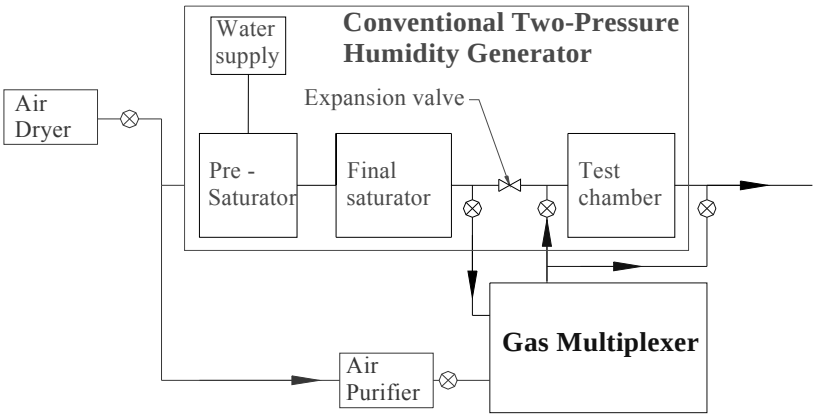

Figure 1. Schematic representation of the Hybrid Humidity Generator (HHG)

The presaturator is a commercially-made system that saturates the incoming gas in a two step process. The gas first passes through a saturation chamber, in which the gas is sprayed with water heated to about 10 °C above T_s. Afterwards the gas passes through the pre-saturator's heat exchanger, which is controlled at approximately T_s. The gas's excess moisture condenses inside this heat exchanger and flows down to the pre-saturator's water reservoir.

The pre-saturator and final saturator are connected using 2.5 cm diameter stainless steel tubing. When T_s is near to or higher than the ambient temperature, the tubing is temperature-controlled to be about 10 °C higher than T_s in order to prevent water condensation in the tubing.

The final saturator is composed of a heat exchanger and saturation chamber. Both systems rest inside a commercially-made temperature-controlled bath of volume 167 L that is uniform to within 0.003 °C at 25 °C. The heat exchanger is located immediately above the saturation chamber in the bath. The gas first enters the heat exchanger, which conditions the gas to be at the temperature of the saturation chamber; this minimizes sensible heat loading on the chamber and also minimizes latent heat loading on it if the entering gas is slightly oversaturated. In addition, the heat exchanger condenses out any moisture above the dew-point of the saturation chamber; this condensed water is then directed down into the saturation chamber. The heat exchanger is made of 316L stainless steel and is composed of two header tanks separated by an array of 116 parallel tubes with inner diameter 7.8 mm and length 48.5 cm. The parallel tube design minimizes the pressure drop across the heat exchanger. The diameter of the tubes is sufficiently large to prevent them from being blocked by condensed water droplets. With the tube dimensions described and with a gas flow of 150 L/min, the gas flows through the parallel tubes for a period of about ten thermal time constants.

The gas exiting the heat exchanger flows into the saturation chamber below. The chamber is flat and roughly rectangular in shape. The saturation chamber is also made of 316L stainless steel and contains a 2.2-cm layer of water and a 2.2 cm layer of gas above it. The chamber has a horizontal area of 0.28 m^2, with total water and gas volumes of 6.16 L each. Stainless steel dividers inside the saturator partition the chamber into two channels of width 3.7 cm that follow a serpentine path, as shown in Fig. 2. Each channel covers half the area of the saturation chamber, as shown. The dividers are continuously welded along their lengths into the top plate of the chamber, allowing no gas flow over the dividers. Twisted vanes are welded to the dividers to improve mixing between the gas and water vapor while the gas is in the saturation chamber.

Inside the saturation chamber, a rectangular cross section rather than a circular cross-section is used because the former exhibits less sensitivity to water height changes than would a circular cross-section design. For a given water level, the rectangular section contains more water volume and has a smaller rate of change in airway cross-sectional area with water level, relative to a circular cross section. Therefore, increases in water volume in the chamber (from water condensation in the heat exchanger) are less likely to restrict the airway; this allows the generator to produce very high dew-point temperatures for significant time periods.

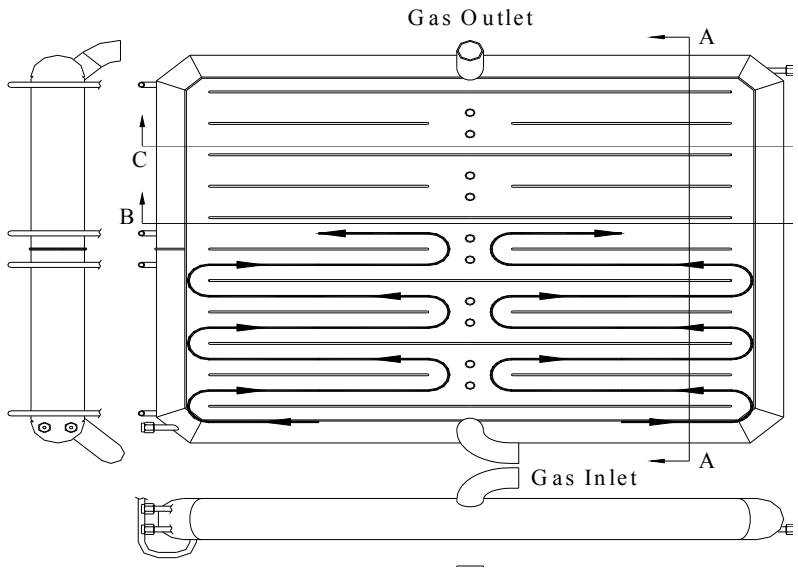

Figure 2. Schematic diagram of the saturation chamber.

After the final saturator was constructed, the stainless steel inside of it was commercially passivated to prevent corrosion and water contamination. Since then, samples of water kept in the saturator for several months have been analyzed and show no noticeable increase in the level of impurities.

A calibrated standard platinum resistance thermometer (SPRT) immersed in the temperature-controlled bath determines the temperature of the final saturator. A computer-interfaced AC resistance bridge, together with a calibrated, temperature-controlled 25 Ω standard resistor, measures the SPRT resistance. The pressure in the saturator is determined using a silicon strain gauge interfaced to a computer; the gauge is connected to a point in the saturator near the gas outlet using ¼ inch (0.635 cm) stainless-steel tubing. This tubing is at a sharp vertical slope in the region immediately above the saturator. Therefore, when the saturator is above the ambient temperature, any condensation occurring in the tubing is directed down to the saturator; this ensures that the transducer is never exposed to condensed water and always properly measures the pressure inside the saturator. Chamber pressure measurements (for dew point determination) are also made with a calibrated silicon strain gauge.

Figure 3 shows the entire heat-exchanger/final-saturator system. On top of the heat exchanger, a horizontal plate supports the system hanging inside the temperature-controlled bath and also serves as the top cover to the bath. Two sets of water fill tubes and gas outlet tubes can be seen in the figure, one for each channel. When viewed from above, the saturator and heat exchanger nearly fill the bath chamber, and almost touch a baffle plate attached to the two bath stirrers (see figure). This configuration promotes optimal circulation of water within the bath, with minimal dead-zones. Such a design minimizes temperature-non-uniformity in the bath.

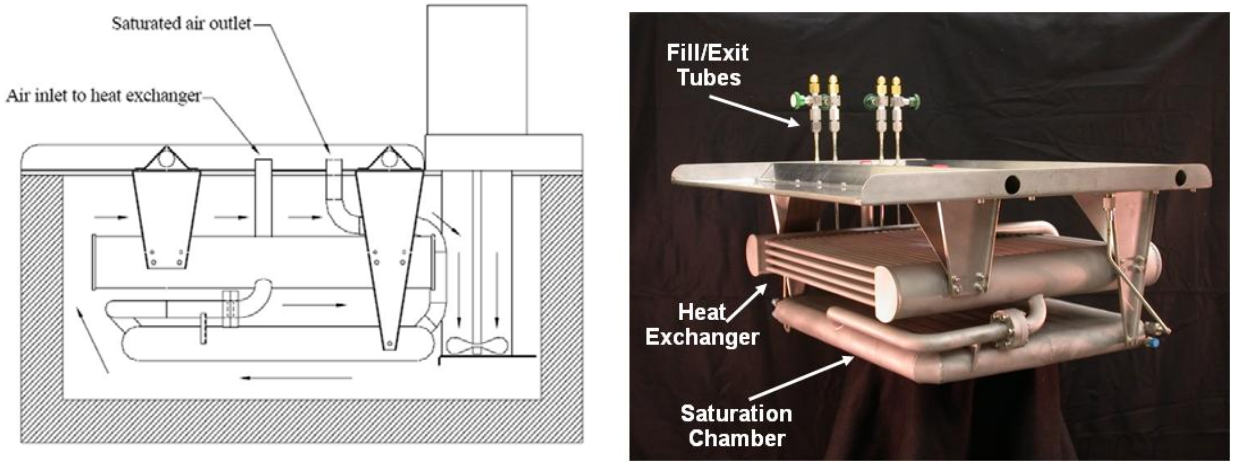

Figure 3. The final saturator. Photograph of the saturator, showing the heat exchanger and saturation chamber (top), and schematic diagram of the saturator in the temperature-controlled bath, showing direction of water flow in the bath (bottom).

The two pressure technique [3] involves saturating the gas at an elevated pressure and afterwards expanding the gas to a lower pressure. The advantage of this technique is that a range of humidity values can be generated using one saturator temperature. This is useful for two reasons. First, it is much faster for an operator to change the saturator pressure than to change the saturator temperature. Secondly, the low humidity limit of the generator is lowered, since the mole fraction is inversely proportional to the saturator pressure.

The HHG employs the two-pressure technique by first using the 550 kPa pressure head of the gas source to raise the pressure in the saturator. It then uses an expansion valve at the exit of the saturation chamber to control the pressure. The expansion valve is a throttle valve with a high-speed motor/gear assembly. A PID controller senses the pressure using the strain gauge mentioned above and controls the opening of the throttle valve. The valve is located immediately above the temperature-controlled bath and is connected to the gas outlet from the saturator.

The divided-flow method [3] involves diluting the saturated gas with dry gas using precisely-metered streams of gas. The mole fraction after dilution is

$$x = \frac{\dot{n}_s\, x_s + \dot{n}_p\, x_p}{\dot{N}} \qquad 2)$$

where $\dot{n}_s$ and $\dot{n}_p$ are the mole flow rates of the saturated gas and pure gas, respectively, and $\dot{N}$ is the total mole flow rate. Also, x_s is the mole fraction of water in the saturated gas and x_p is the residual mole fraction of water in the pure gas. Such a technique allows generation of arbitrarily low humidity values while operating the saturator at convenient temperatures. When generating low humidity, this method has three principal advantages. First, the temperature-controlled bath may be operated with water, which is much safer and less expensive than liquids with lower

freezing temperatures. Secondly, the technique allows the generator to avoid the large temperature gradients in the bath that often exist at low temperatures; these gradients add large uncertainties to the uncertainty of the generated humidity. Finally, the saturation occurs near the triple point of water, a temperature at which the water vapor pressure is well known.

The HHG employs the divided-flow method using a gas multiplexer, shown in Figure 4. The multiplexer contains seven flow-metering banks. Each bank consists of a commercially-made mass-flow controller and a commercially-made flow meter (a laminar-flow element). The flow meters cover the range from 1 cm^3/min to 100 L/min. The upstream side of each flow bank connects in parallel to both the saturated gas supply and a purified gas supply. When the divided flow method is used, both the saturated gas supply (and hence the saturator) and the purified gas are kept at a pressure of approximately 300 kPa. The purified gas comes from the original gas source (described at the beginning of this section), but it is additionally dried using a molecular sieve specified to reduce the water mole fraction of the gas to 1×10^{-9}. The downstream side of each flow bank connects to a common outlet manifold. Pneumatic valves controlled by a computer select whether dry gas, wet gas, or no gas flows through each bank. For those banks with flow, the computer-controlled mass-flow controllers adjust the flow to provide the dilution nominally specified. The flow meters measure the exact flows and provide this information to the computer. These flow meters have been calibrated by the NIST Fluid Metrology Group, using upstream pressures of 300 kPa to replicate the conditions under which they are used.

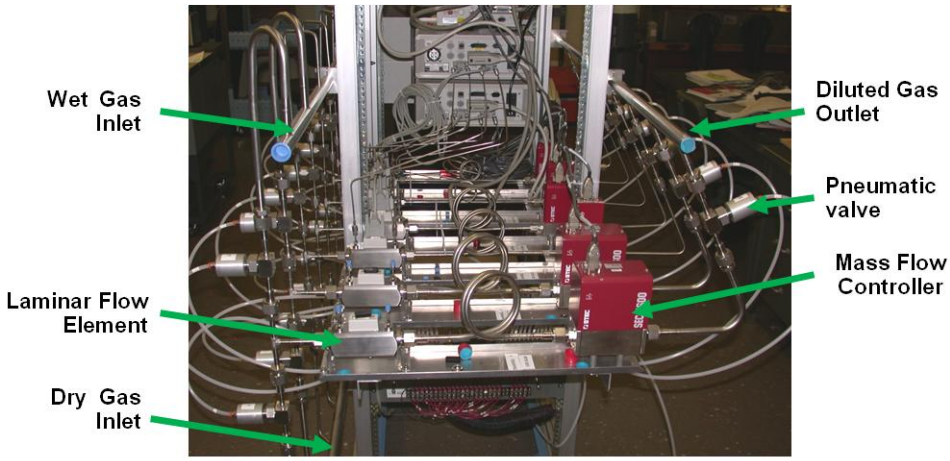

Figure 4. The gas multiplexer, which is used when the HHG is operated in divided-flow mode.

5. Uncertainty Budget

We have performed a series of performance and validation tests on the HHG, which are described elsewhere. [2] The performance tests include measurements of temperature non-uniformities inside and immediately outside the final saturator under various conditions (e.g., variations in bath temperature, gas-flow rate, and dew-point differences between the pre-saturator and final saturator). Other performance tests involve measurements of pressure

stability in the final saturator under various pressures and gas-flow rates. Finally, performance tests have been conducted to determine the self-consistency of the two-pressure method as well as the dilution method. Based on these performance tests as well as measurement equipment specifications, we have constructed uncertainty budgets for the humidity generated by the HHG. There are budgets for the two expressions of humidity (mole fraction and dew/frost-point) under two conditions: two-pressure generator without dilution and two pressure with dilution. The total uncertainties associated with these budgets are based on the ISO and NIST guidelines for the expression of uncertainty in measurement [10,11].

In Figures 5 to 7, the total uncertainty for humidity generated by the hybrid generator is presented for four cases: 1) water mole fraction generated directly from the saturator (no dilution), 2) dew-point temperature generated directly from the saturator (no dilution), 3) water mole fraction when the generator is used in 2-P mode and divided-flow mode, and 4) frost-point temperature when the generator is used in 2-P mode and divided-flow mode. In the figures, P_c is the pressure in the test chamber. Also, e_s^{calc} and e_c^{calc} refer to the vapor-pressure relations $e(T_s)$ and $e(T_c)$ (where T_c, is the temperature in the test chamber), respectively, and f_s^{calc} and f_c^{calc} refer the enhancement factor relations $f_s(T_s,P_s)$ and $f_s(T_c,P_c)$, respectively; these quantities all have uncertainty due to the imperfect knowledge of their physical relations. The figures do not contain all uncertainty elements for the calibration of hygrometers by the HHG, as they do not include uncertainties from measurement repeatability of the particular hygrometer under calibration. Ref. [2] presents a table with an uncertainty budget and discusses many of the uncertainty components values.

Figure 5 shows the total expanded uncertainty for humidity generated by the HHG when the generator is operated in 1-P mode. The uncertainty is shown for the a) mole fraction (relative uncertainty) and b) dew point. Here, the total expanded uncertainty is given by $U(x) = ku(x)$, where the coverage factor is $k = 2$. The expanded relative uncertainty is given by $U_r(x) = U(x)/x$. In the figure, the black curve represents the total uncertainty, while the other curves represent the contributions to the total uncertainty from individual uncertainty components. In Fig. 5(b), the uncertainty contributions from e_s^{calc} and e_c^{calc} are zero, because these uncertainties are cancelled out when the generator is used in 1-P mode; the uncertainty contributions for f_s^{calc} and f_c^{calc} are zero for the same reason. Also in this plot, the curve designated as "*P*" represents the contributions from both P_s and P_c. The figure shows that for the 1-P mode, the dominant uncertainty is from pressure measurement and stability, except for saturator temperatures above 60 °C; in this case uncertainties due to temperature non-uniformities in the bath dominate. Figures 6(a) and 6(b) show similar plots for the case when the generator is operated in 2-P mode with P_s = 500 kPa. In Fig. 6(b), the discontinuity at 0 °C is due to the assumption of frost-point generation below this temperature. This figure shows that when the saturator is operated in this way, the uncertainties in f_s^{calc} and f_c^{calc} usually dominate.

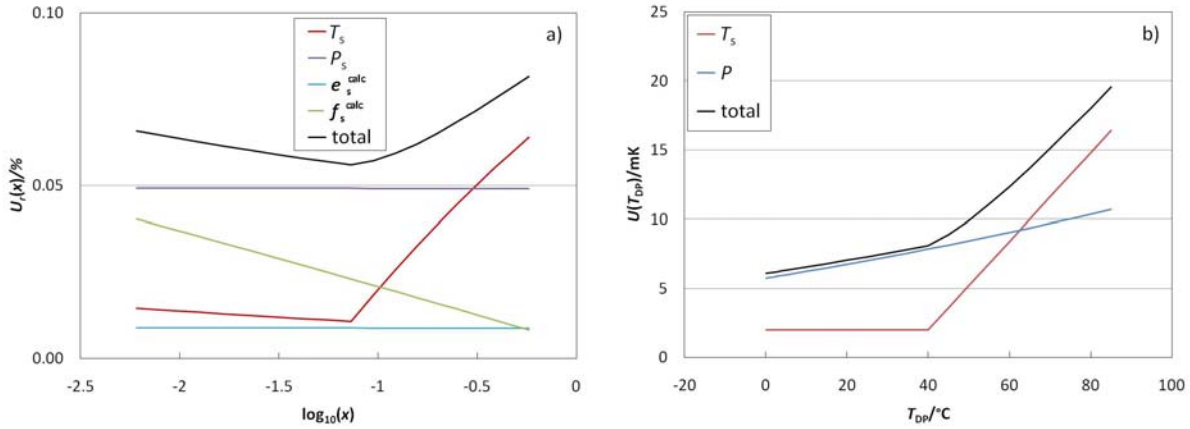

Figure 5. Total expanded uncertainty U for the (a) mole fraction and (b) dew-point temperature generated by the HHG saturator when used in 1-P mode. The black curve represents the total uncertainty, while the other curves show the contributions from individual uncertainty elements. In a), the expanded uncertainty is expressed as a relative uncertainty $U_r(x) = U(x)/x = ku(x)/x$, where $k = 2$ and $u(x)$ is the standard uncertainty for x. In b), the total expanded uncertainty is $U(T_{DP}) = ku(T_{DP})$. In b), P represents the combined contributions from both P_s and P_c.

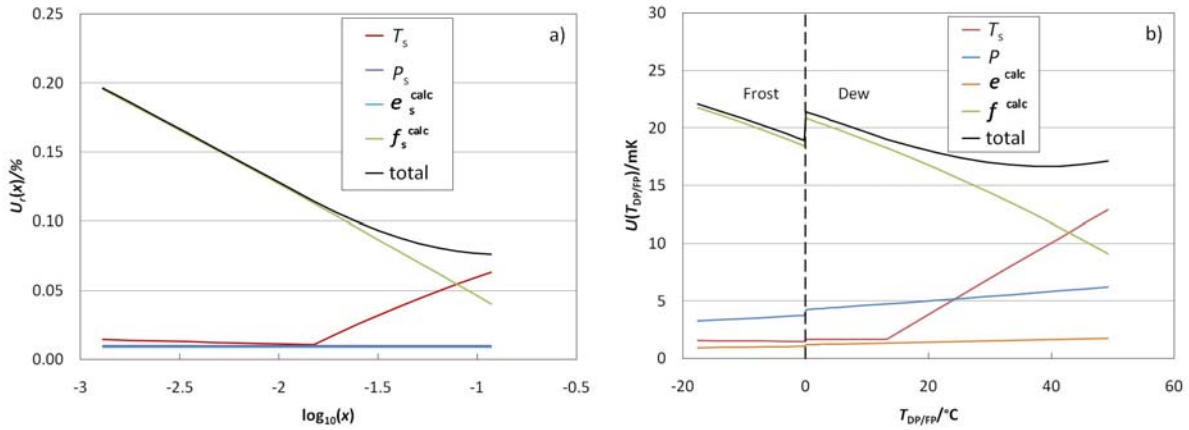

Figure 6. Total expanded uncertainty U for the (a) mole fraction and (b) dew/frost-point temperature generated by the HHG saturator when used in 2-P mode with P_s = 500 kPa. The black curve represents the total uncertainty, while the other curves show the contributions from individual uncertainty elements. In a), the expanded uncertainty is expressed as a relative uncertainty $U_r(x) = U(x)/x = ku(x)/x$, where $k = 2$ and $u(x)$ is the standard uncertainty for x. In b), the total expanded uncertainty is $U(T_{DP}) = ku(T_{DP})$. In b), P , e^{calc}, and f^{calc} each represent the combined contributions of their quantity from both the saturator and chamber (hygrometer).

Figure 7 shows the expanded uncertainty generated by the HHG when it is used in divided-flow mode. The uncertainties plotted are (a) the water mole fraction (relative uncertainty) and (b) the frost-point temperature. For these plots, the saturator parameters are $P_s = 300$ kPa and $T_s = 0.5$ °C. In the plots, "*n*" refers to the combined contribution to the total uncertainty from n_s and n_p. In Fig 7(a), $U_r(x)$ is relatively constant for $x > 2{\cdot}10^{-5}$. At the highest value of x shown in the plot, $\dot{n}_p = 0$ and so $U_r(x)$ is only due to the saturator. As x decreases to $2{\cdot}10^{-5}$, $U_r(x)$ increases slightly due to the rising significance of $u(\dot{n}_s)$ and $u(\dot{n}_p)$. As x decreases below $2{\cdot}10^{-5}$, $u(x_p)/x$ dominates $U_r(x)$, increasing its value to nearly 1% at $x = 2{\cdot}10^{-6}$. In (b), the total expanded uncertainty is $U(T_{FP}) = ku(T_{FP})$. For -55 °C $\le T_{FP} \le -12$ °C, $U(T_{FP}) \approx 14$ mK and is relatively constant over this entire range. As T_{FP} decreases below −55 °C, $U(T_{FP})$ rises rapidly up to 58 mK at −70 °C due to the increasing influence of $u(x_p)$.

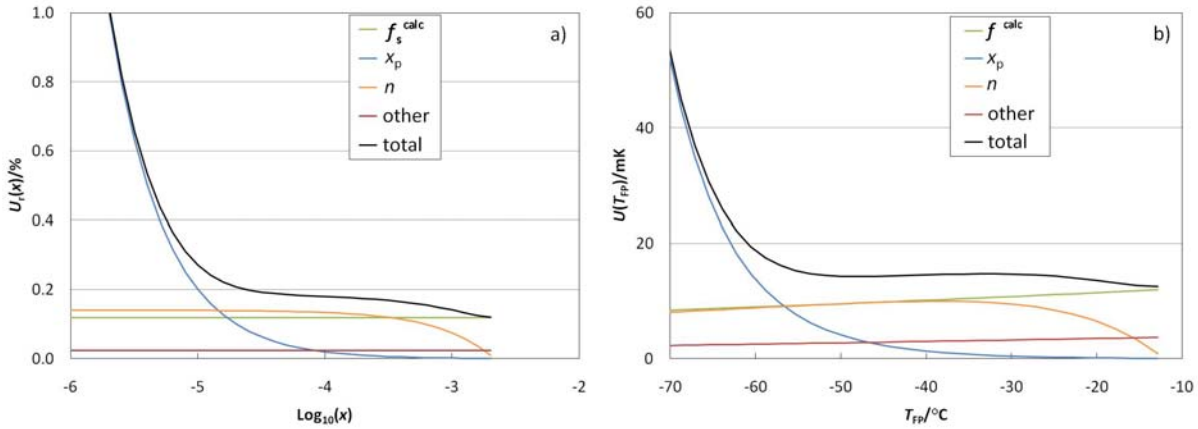

Figure 7. Total expanded uncertainty for the a) water mole fraction (relative uncertainty) and b) frost-point temperature generated by the HHG when it is used in divided flow mode with a saturator pressure of $P_s = 300$ kPa.

6. Comparisons with other NIST Generators

To further validate the performance of the HHG and also determine the level of consistency between the NIST thermodynamic humidity generators, we made comparison measurements with the NIST 2-P generator [5] and the LFPG [6]. One set of comparisons was performed using an uncalibrated chilled-mirror hygrometer as a transfer standard. For the dew points generated, the expanded uncertainties (k=2) for the 2-P generator and LFPG are 40 mK [5] and 13 mK [6], respectively. In the LFPG, nitrogen was used as the gas source. Figure 8 shows the difference between the measured dew point and the expected dew point from the generator over the range −15 °C to 30 °C. For measurements below 0 °C, the gas moisture was observed to condense on the mirror as dew rather than frost. The HHG and LFPG agree within 10 mK, which is within the combined expanded uncertainties of the two generators and the hygrometer. The HHG and 2-P generator agree within 40 mK; the difference is also within their combined expanded uncertainties, though only marginally so. A second set of comparison measurements was made against the LFPG over the frost point range −50 °C to −20 °C using a second chilled-mirror hygrometer. The comparison values and respective expanded uncertainties are shown in Figure 9. Once again, the HHG and LFPG agree within the combined expanded uncertainties of the two

generators and the hygrometer over this range. Finally, a third set of comparison measurements was made against the LFPG over the low-humidity range. This time the comparison was made using a commercial cavity ring down spectrometer as the transfer standard hygrometer. The humidity unit measured was water mole fraction. The measurements were made over the range 1 µmol/mol to 5 µmol/mol (−76 °C to −65 °C frost point). To simplify the comparison, air was used as the gas source in the LFPG as well as in the HHG. The results shown in Figure 10 agree to within the generators' expanded uncertainties. The results of these comparisons validate the performance of the HHG, showing that it generates correct humidity values to within its uncertainties.

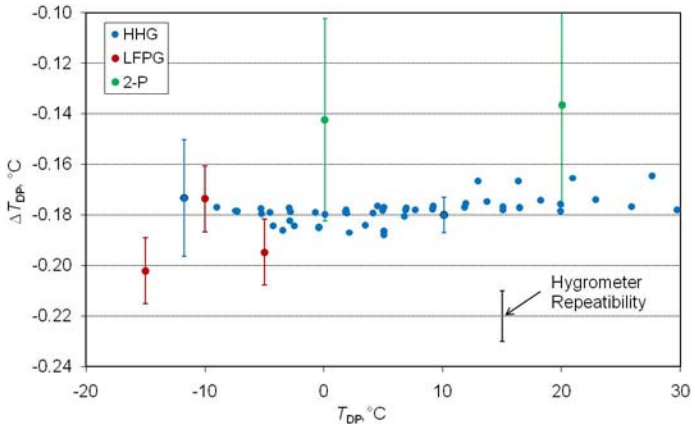

Figure 8. Comparison of dew points generated by the HHG with those generated by the NIST Two-pressure (2-P) generator and the NIST Low Frost-point Generator (LFPG). The comparisons were made using an uncalibrated chilled-mirror hygrometer as a transfer standard. Here, $\Delta T_{DP} = T_{DP\text{-}g} - T_{DP\text{-}h}$, where $T_{DP\text{-}g}$ is the dew point expected from the generator and $T_{DP\text{-}h}$ is the dew point measured by the hygrometer. The uncertainty bars reflect the expanded (k=2) uncertainties of the generators and hygrometer.

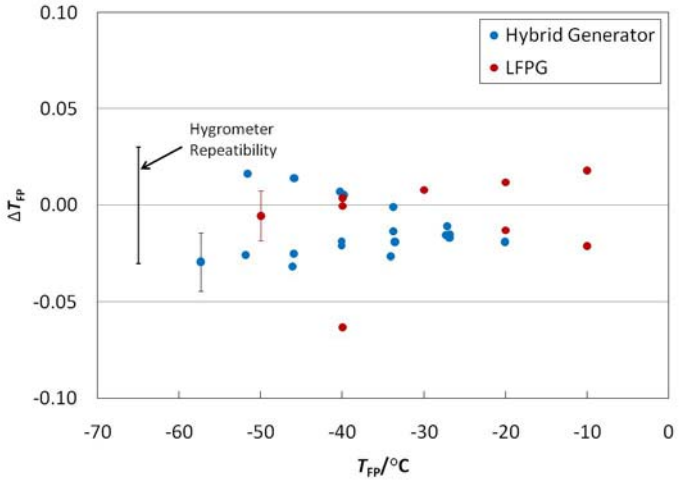

Figure 9. Comparison of frost points generated by the HHG with those generated by the LFPG. The comparisons were made using a second chilled-mirror hygrometer as a transfer standard. Here, $\Delta T_{FP} = T_{FP\text{-}g} - T_{FP\text{-}h}$, where $T_{FP\text{-}g}$ is the frost point expected from the generator and $T_{FP\text{-}h}$ is the frost point measured by the hygrometer.

7. Summary

We have described here the design and performance of the new hybrid generator at NIST, which generates dew/frost-points between −70 °C and 85 °C (mole fractions between 2.5 µmol/mol and 0.57 mol/mol). This primary generator uses a novel design that incorporates both the two-pressure method and divided-flow method; this provides an opportunity to perform validation tests on the conventional 2-P method in the low-frost-point range. Between −60 °C and 85 °C the dew/frost-point expanded uncertainty is always below 25 mK. Between −70 °C and −60 °C the uncertainty is between 25 mK and 60 mK. Over the low frost point range, this uncertainty is considerably lower than the uncertainty of most 2-P generators, including that of NIST. Over the range −70 °C to −60 °C, the uncertainty of the HHG is larger than over higher ranges due to the increasing influence of the uncertainty of x_p (see Fig. 7), which we estimate to be $u(x_p)$ = 10 nmol/mol; however, this uncertainty may be lowered as methods are developed to accurately measure this mole fraction. Comparison of the expected humidity generated by the HHG with that by other NIST generators shows agreement within the expanded uncertainties of the generators and transfer hygrometer, validating the performance of the HHG.

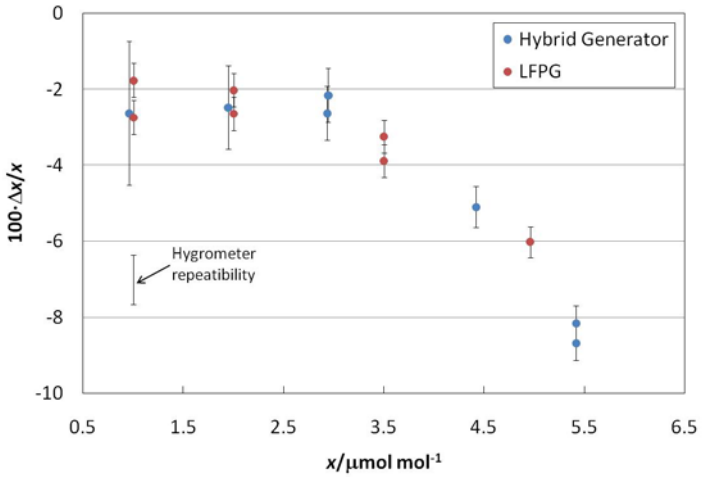

Figure 10. Comparison of mole fraction x generated by the HHG with that generated by the NIST Low Frost-point Generator. The comparisons were made using a commercial cavity ring down spectrometer as a humidity transfer standard. Here, $\Delta x = x_g - x_h$, where x_g is the mole fraction expected from the generator and x_h is the mole fraction measured by the hygrometer. The uncertainty bars reflect the expanded (k = 2) uncertainties of the generators.

Published in Proceedings of NCSLI 2008 Workshop and Symposium (Boulder, CO: NCSLI, 2008), on CD

References

1. G.E. Scace et al., An Overview of the NIST Hybrid Humidity Generator, in Proceedings of the 5th International Symposium on Humidity and Moisture, in print.

2. C.W. Meyer et al, Performance and Validation Tests on the NIST Hybrid Humidity Generator, in Proceedings of the 10th International Symposium on Temperature and Thermal Measurements in Industry and Science (TEMPMEKO 2007), Int. J. Thermophys., DOI 10.1007/s10765-007-0342-4.

3. A. Wexler, Humidity Standards, Tappi **44** (6), 180A −191 A (1961).

4. S. Hasegawa and J.W. Little, The NBS Two-Pressure Humidity Generator, Mark 2, Jour. Res. NBS **81A**, 81−88 (1977).

5. P.H. Huang, Determining Uncertainties of Relative Humidity, Dew/frost-point Temperature, and Mixing Ratio in a Humidity Standard Generator, in Papers and Abstracts from the Third International Symposium on Humidity and Moisture, National Physical Laboratory, Teddington, UK (1998), 149-158.

6. G.E. Scace and J.T. Hodges, Uncertainty of the NIST Low Frost-point Humidity Generator, in Proceedings of TEMPMEKO 2001: the 8th International Symposium on Temperature and Thermal Measurements, B. Fellmuth, J. Seidel, G. Scholz, eds., VDE Verlag GmbH, Berlin (2002), 597-602.

7. A. Saul and W. Wagner, International Equations for the Saturation Properties of Ordinary Water Substance, J. Phys. Chem. Ref. Data **16,** 893−901 (1987).

8. W. Wagner and A. Pruss, International Equations for the Saturation Properies of Ordinary Water Substance--Revised According to the International Temperature Scale of 1990, J. Phys. Chem. Ref. Data **22**, 783−787 (1993).

9. R.W. Hyland and A. Wexler, Formulations for the Thermodynamic Properties of Dry Air from 173.15 K to 473.15 K, and of Saturated Moist Air from 173.15 K to 372.15 K, at Pressures to 5 MPa., ASHRAE Trans. **89-IIa**, 520−535 (1983).

10. ISO, Guide to the Expression of Uncertainty in Measurement, International Organization for Standardization, Geneva (1993).

11. Taylor B.N. and Kuyatt C.E., Guidelines for Evaluating and Expressing the Uncertainty of NIST Measurement Results, NIST Technical Note 1297, National Institute of Standards and Technology, Gaithersburg (1994).